# Microwave gas sensor based on graphene aerogel for breath analysis

Gabriele Restifo Pecorella
*Dept. of Engineering*
*University of Palermo*
Palermo, Italy

Gianluca Verderame
*Dept. of Engineering*
*University of Palermo*
Palermo, Italy

Patrizia Livreri
*Dept. of Engineering*
*University of Palermo*
Palermo, Italy

Antonio Lombardo
*London Centre for Nanotechnology and*
*Dept. of Electronic and Electrical Engineering*
*University College of London*
London, United Kingdom
corresponding author: a.lombardo@ucl.ac.uk

***Abstract*—Exhaled breath can be used for early detection and diagnosis of diseases, monitoring metabolic activity, and precision medicine. In this work, we design and simulate a microwave sensor in which thin graphene aerogels are integrated into rectangular microwave waveguides. Graphene aerogels are ideal sensing platforms for gases and volatile compounds as they combine extremely high surface-to-volume ratio and good electrical conductivity at RF and microwave frequencies. The latter is modified by exposure to different gases, and -when integrated into a waveguide- these changes result in significant shifts in transmission and reflection scattering parameters. We model the aerogel as a graphene grid with hexagonal openings of size 22.86x10.16x0.1 mm$^3$, characterized by an air volume equal to about 90% of its entire volume. This grid is used as a building block for modeling thicker samples (up to 9 mm). To simulate the variation in the dynamic conductivity of the graphene sheets as a consequence of the absorption of gaseous molecules, a sweep of the chemical potential from 0.0 eV to 0.5 eV with steps of 0.1 eV was used. The results show a significant variation of the waveguide transmission scattering parameters resulting from the gas-induced modification of the graphene conductivity, and hence the potential of the proposed sensor design for breath analysis.**

***Index Terms*—graphene aerogel, gas sensors, rectangular waveguide, microwave sensors.**

## I. Introduction

Exhaled breath contains over 1,000 different biomarkers, which can be either volatile organic compounds (VOCs) or aerosol particles [1]. The analysis of such compounds and particles can be used for early detection and diagnosis of diseases, monitoring metabolic activity and precision medicine. The chemicals present in the breath provide information not only related to the respiratory or digestive systems but also reaching the lungs from another part of the body via the bloodstream. Through the analysis of volatile biomarkers, various diseases can be identified such as cancer, respiratory tract infections, diabetes, intolerances, asthma, inflammation as well as the detection of drug use [1], [2]. For example, breath analysis has successfully been used in pilot studies as alternative to polymerase chain reaction (RT-PCR) to identify patients infected with SARS-CoV-2 virus [3]. Moreover, breath analysis has a high potential for point of care diagnostic, as it is not invasive, collection of samples does not require specialized training and can be repeated as often as required.

Breath analysis is based on the identification of biomarkers present in VOCs and aerosol particles using techniques such as gas chromatography with mass spectrometry (GC-MS) [4], ion mobility spectrometry (IMS) [5], proton transfer reaction mass spectrometry (PTR-MS) [6] and selected ion flow tube-mass spectrometry (SIFTMS) [7]. Such techniques provide very high sensitivity, however, they require exhaled breath to be sampled and delivered to specialized laboratories equipped with bulky and expensive equipment, thus limiting the application of breath analysis in applications such as point of care diagnostic, precision medicine and continuous monitoring of metabolic activity. Therefore, portable solutions are needed to release the full diagnostic and monitoring potential offered by breath analysis. Such solutions should combine a small footprint, low manufacturing cost and integrability with existing technologies, in particular the ubiquitous platform offered by information and telecommunication technology.

Mimicking the human olfactory system, a possible solution is represented by arrays of gas sensors that allows identification and analysis of different VOC molecules. Given this similarity, this type of sensors are called electronic noses ("e-noses") [9]. Among these sensor arrays, the most successful are chemoresistive and resonant quartz devices which showed success rates in identifying gas molecules that reflect the presence of various types of cancer and different diseases [10]–[15]. Breath analysis can also be carried out with the use of Field Asymmetric Ion Mobility Spectrometry (FAIMS). This technology, which allows the real-time separation of the profiles of VOC molecules [17], is based on the application of an alternating electric field across the ion path of a sample vapor via an alternating voltage applied to two parallel plates. The result is a filter that allows only certain ions to pass through, at atmospheric pressure and room temperature. [16], [17].

An alternative and less explored approach to gas sensing is provided by microwave sensors. Microwaves are a powerful tool for fingerprinting materials and molecules via their frequency-depended interaction with electromagnetic waves propagating in a suitable waveguide or resonant circuit. They interact with matter by causing frequency-dependent reorientation motion of molecular dipoles and translation motion of ions and electrons, enabling identification of specific molecules and compounds. Microwave sensors can be divided into two categories depending on their operating frequency range: narrow-

band and broadband. Narrow-band sensors usually consist of resonators, whose resonance frequency is modified by the exposure to analytes. Broadband sensors are realized using waveguides such as coplanar or microstrips. The material to be tested is placed near of the waveguide, and its interaction with the fringe field causes variations in the propagation and reflection parameters, and it is the method of choice for broadband dielectric spectroscopy [18].

Microwave sensors typically consist of metallic structures and the interaction between sensor and analyte is entirely due to the modification of the dielectric environment due to the proximity of the molecules and compounds and the top side of the waveguides. Graphene consists of a single layer of carbon atoms tightly packed in a hexagonal lattice. This structure leads to a linear gapless energy dispersion, rendering graphene as a semimetal with tunable charge carrier density and type (electron and holes). The tunability of charge carriers density is accompanied by a good DC and RF/microwave conductivity, making it a very interesting candidate for microwave sensing. Indeed, chemical doping due to absorbates on its surface, cause significant changes in its conductivity, enhancing the sensitivity compared to microwave metallic sensors, where the sensing mechanism is entirely due to changes in permittivity of the gas/material on top of the waveguide. Of particular interest for breath analysis are graphene aerogels (GAs), which consist of graphene layers arranged in a three-dimensional structure with extremely high porosity [19]. Aerogel materials are characterized by an extremely low density (almost identical to that of air), large Brunauer-Emmett-Teller (BET) specific surface area and are ultralight [21], [22]. In addition, graphene-based aerogels show good electrical conductivity which, combined with their highly porous structure, make them ideal materials for breath sensors. Graphene aerogels are typically produced by freeze-drying. This method consists in the rapid freezing of a graphene dispersion, which "locks" the graphene flakes in a three-dimensional structure. The frozen solvent is then removed by sublimation, leaving the graphene flakes to form a porous structure [20].

In this work, we design and simulate a sensor for breath analysis by integrating different graphene aerogels within rectangular waveguides having suitable gas inlet and outlet. We simulate the devices using CST Studio Suite 2021 at frequencies $8 \div 12$ GHz and investigate how variations of chemical doping in the graphene layers forming the aerogel are reflected in the transmission parameters of the waveguide. In order to reflect the non-periodic, highly porous structure of the aerogel, we define a 100-µm thick grid as "building block" and we model the three-dimensional aerogel as a stack of grids with a random lateral shift. We observe significant modification and non-trivial trends in the transmission parameters as function of graphene chemical potential, showing the potential of these devices for breath analysis.

## II. The use of graphene for breath analysis

### A. Graphene transport properties at RF and Microwave

The dynamic conductivity of single-layer graphene is described starting by the Kubo formalism for magnetic and conduction problems [23]. It can be expressed as [24]:

$$\begin{aligned}\sigma(\omega) &= \sigma_{intra}(\omega) + \sigma_{inter}(\omega) = \\ &= \frac{2e^2T}{\pi\hbar}\frac{i}{\omega + i\tau^{-1}}\log\left[2\cosh\left(\frac{E_F}{2k_BT}\right)\right] \\ &+ \frac{e^2}{4\hbar}\left[H\left(\frac{\omega}{2}\right) + \frac{4i\omega}{\pi}\right. \\ &\left.\times\int_0^\infty \partial\epsilon\frac{H(\epsilon) - H(\omega/2)}{\omega^2 - 4\epsilon^2}\right]\end{aligned} \tag{1}$$

where $\omega = 2\pi f$ is the angular frequency, $\mu_c$ the Fermi energy (also called chemical potential), $\tau$ the scattering time assumed to be independent of energy, $T$ is the temperature expressed in Kelvin, $e = 1.6 \cdot 10^{-19}\ C$ is the electron charge, $\hbar = \frac{h}{2\pi}$ is the reduced Planck's constant, $k_B = 1.38 \cdot 10^{-23}\ \frac{J}{K}$ the Boltzmann's constant. $H(\epsilon)$ is given by [24]:

$$H(\epsilon) = \frac{\sinh\left(\frac{\hbar\epsilon}{k_BT}\right)}{\cosh\left(\frac{E_F}{k_BT}\right) + \cosh\left(\frac{\hbar\epsilon}{k_BT}\right)} \tag{2}$$

where $\epsilon$ is the characteristic electron energy. Relation (1) is composed of two contributions: intraband and interband contribution, respectively. The chemical potential is determined by the charge of carriers density $n_s$, which can be expressed as [26]:

$$n_s = \frac{2}{\pi\hbar^2 v_F^2}\int_0^\infty E[f_d(E) - f_d(E + 2E_F)]dE \tag{3}$$

From DC to microwave frequencies, for typical values of $\mu_c$, the energy of the electromagnetic waves is insufficient to promote an electron from the valence band to the conduction band (interband transition) and the following condition exists $\hbar\omega < 2|\mu_c|$ [24]–[27]. Therefore, for the purpose of this work, in expression (1) it is possible to neglect the interband conductivity term and express the dynamic conductivity of graphene only through the contribution of intra-band conductivity which can be expressed as [26]:

$$\begin{aligned}\sigma_{intra}(\omega, E_F, \tau, T) &= \\ &= -i\frac{e^2k_BT}{\pi\hbar^2(\omega - i\tau^{-1})}\left[\frac{E_F}{k_BT} + \right. \\ &\left. + 2ln\left(1 + e^{-\frac{E_F}{k_BT}}\right)\right]\end{aligned} \tag{4}$$

Equation (4) shows how changes in Fermi level (chemical potential) induced by molecules or compounds absorbed on the graphene surface modify its DC and AC conductivity, leading to modification of wave transmission. This effect results in a

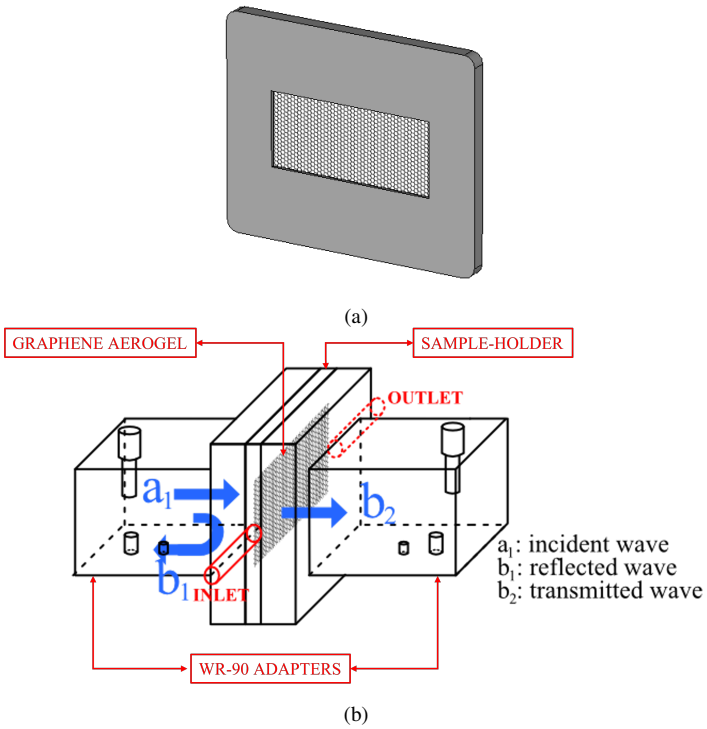


Fig. 1. (a) Designed graphene aerogel inserted in a holder. (b) Schematic view of the designed sensor: The sample holder is sandwiched between two coax-to-WR90 adapters and two tubular channels are inserted in the holder to obtain a gas inlet and outlet.

double sensing mechanism: on one hand the wave propagating along the waveguide directly interacts with the gas trapped in the aerogel and on the other the gas modifies the conductivity of the aerogel, resulting in enhanced sensitivity.

### *B. Graphene doping via adsorbates*

The modulation of the Fermi level in graphene occurs through electron or hole injection for n-type and p-type doping, respectively. The adsorption of doping impurities on the surface allows keeping the honeycomb structure of graphene intact with surface charge transfer. The excellent electrical, chemical and physical properties are thus preserved when compared to a substitution of doping impurities [28]. The type of doping to be obtained must be sought in the graphene Fermi level position concerning the summit of the adsorbate valence band [29]: when the Fermi level is under this summit the gas molecule acts as a donor (n-type doping) while when the Fermi level is above the gas molecule acts as acceptor (p-type doping). Therefore, the doping induced by the adsorption of the gaseous molecules on the surface of the two materials involves changes in the surface conductivity $\sigma$. Studies on gaseous molecules commonly present in the air have shown that molecules such as $NH_3$, $CO$ act as donors while molecules such as $O_2$, $H_2O$, $NO_2$ act as acceptor atoms [30], [31].

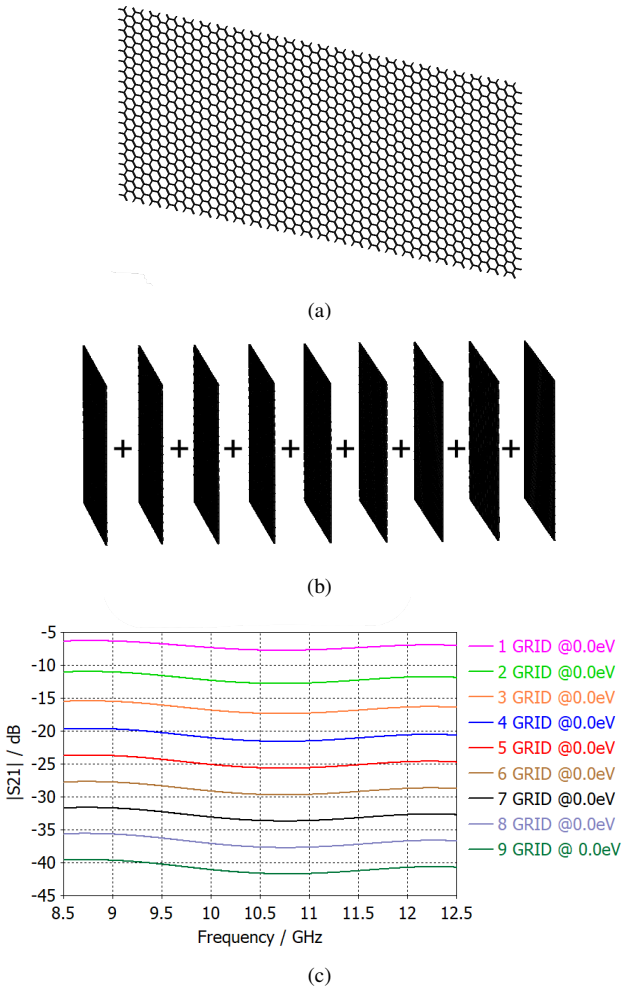


Fig. 2. (a) A three-dimensional hexagonal graphene grid with a 100 µm thickness. (b) This grid was later added to another grid to obtain a greater thickness. This operation was carried out 9 times until a total thickness of 900 µm (9 layers) was obtained. (c) Simulated transmission coefficient for a different number of grids and chemical potential equal to 0.0 eV. From the figure, it can be noted that increasing the overall GA thickness results in a decrease of the transmission coefficient due to an increased EM absorption. Therefore, the optimal overall thickness value should be less than 0.5 mm (5 grids).

## III. Sensors Design

The designed sensor consists of a graphene aerogel sample interposed between two rectangular waveguide (WR) parts. The chosen WR has the standard dimensions of a WR90 with a fundamental mode frequency ($f_{TE_{10}}$) of 6.557 GHz. In order to work only with the fundamental mode, the chosen working frequency range is $8 \div 12$ GHz. In addition, we designed a holder for the aerogel sample. The sample holder has two openings whose area is equal to the section of the WR90 (22.86 x 10.16 mm$^2$), as shown in figure 1(a). The holder containing the graphene aerogel sample is positioned in the centre of the structure to obstruct the propagation of electromagnetic waves according to the scheme shown in the Fig. 1(b).

To create material in CST Studio Suite 2021 with a large surface-to-volume ratio that does not involve excessive com-

putational time, we designed a 100 µm thick three-dimensional hexagonal grid and modelled the conductivity of the materials forming the grid according to equation (4). We assume pristine single-layer graphene with a scattering relaxation time of 0.1 ps at 300 K. In the first approximation, we assume that the scattering relaxation time is not significantly altered by the chemical doping.

The designed "building block" grid is shown in Fig. 2(a) and is characterized by an air volume corresponding to approximately 90% of its total volume (22.86x10.16x0.1 $mm^3$). Our building block grid allows us to study the effect of aerogel thickness and identify the range that maximized the sensing without blocking the wave propagation. To do so, we simulated the scattering parameters for a number of randomly-misaligned grids ranging from 1 to 9, for a total thickness of the graphene aerogel ranging from 100 µm (one grid) up to 900 µm (nine grids), as shown in Fig. 2(b). Looking at Fig. 2(c) it is possible to note that simulations results showed good transmission response of the designed sensor for an overall thickness not exceeding 500 µm. Beyond this thickness, due to a large EM absorption by the GA, the transmission coefficient becomes extremely small ($\sim$ -40 dB) and therefore this thickness represents an upper limit for aerogels that can be used for the proposed sensor.

## IV. Simulation Results

When the surface of single-layer graphene is exposed to gaseous molecules, these are adsorbed onto it resulting in a p- or n-type doping depending on their nature. To investigate its response, the designed sensor was numerically simulated using the CST Studio Suite 2021 software. For the simulations, the air was chosen as background material and to simulate changes in the building-block graphene dynamic conductivity due to the adsorption of gas or molecules, a sweep of its chemical potential was simulated. In particular, the chemical potential was varied from 0.0 eV to 0.5 eV with steps of 0.1 eV while maintaining constant to 0.1 ps the scattering relaxation time. The range of chemical potential has been chosen to reflect variations of chemical potential experimentally observed [30], [32] as well as unintentional chemical doping usually exhibited by graphene. Changing the chemical potential results in a sensor response which is characterized by changes in its scattering parameters i.e., reflection and transmission coefficient. It should be noted that we are only considering the changes in graphene conductivity and neglecting the effect of direct interaction of the gas with the propagating wave. In an experimental implementation of our design, the presence of the gas within the voids in the aerogel and in the waveguide would also modify the wave propagation, thus provide an additional sensing mechanism and potentially higher sensitivity. Figs. 2(c) illustrates the simulated transmission coefficient for three different total thicknesses of the graphene aerogel, 100 µm, 400 µm and 900 µm, respectively. The amplitude of the transmission coefficient linearly depends on the thickness of the graphene aerogel sample: with a large thickness, small values of $|S_{21}|$ are obtained and vice versa.

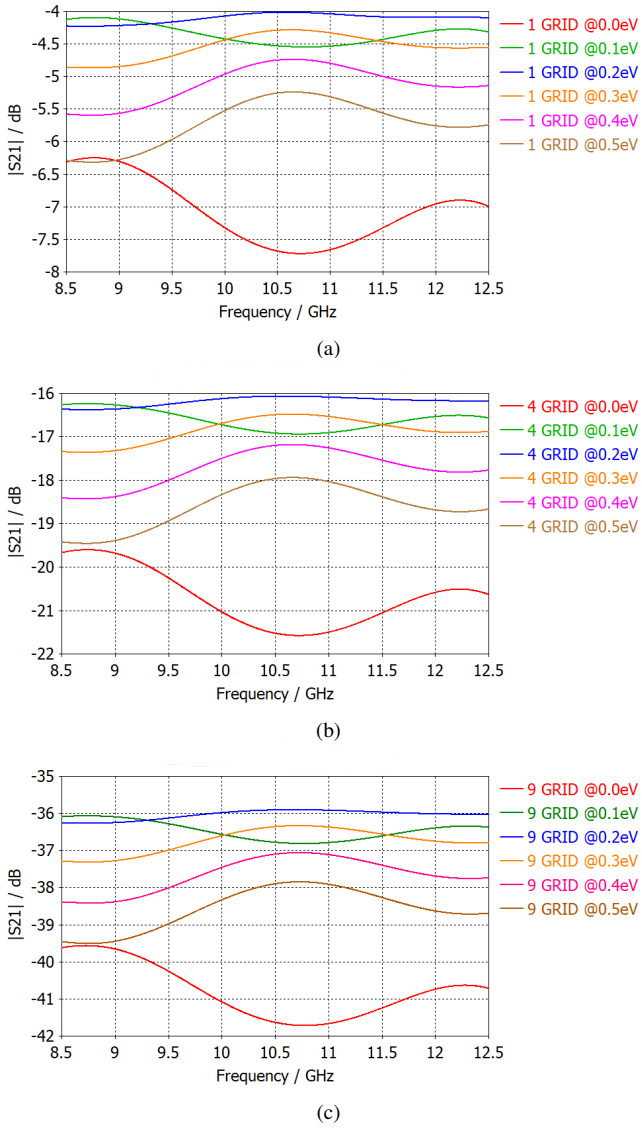


Fig. 3. Simulated transmission coefficient of the designed sensor for three different scenarios. The overall GA thickness is equal to 100 µm in (a), 400 µm in (b) and 900 µm in (c). To simulate the absorption gaseous molecules by GA sample, a sweep of the chemical potential from 0.0 eV to 0.5 eV with steps of 0.1 eV was performed for all scenarios.

Then, we simulate the effect of varying chemical potential for sensors having three different aerogel thicknesses, respectively 100, 400 and 900 µm i.e., 1, 4 and 9 grids. The simulation results, shown in Fig. 3 (a-c), show that for all thicknesses the minimum value of the transmission coefficient is obtained for a chemical potential equal to 0.0 eV (red lines) at $\sim$10.75 GHz. The same trend is obtained for 0.1 eV (green lines) but with a significantly increased minimum value. For chemical potential higher than 0.1 eV, the concavity of its transmission coefficient is different and there is a decrease in the modulus as the chemical potential increases.

In other words, by increasing the conductivity, the rectangular waveguide tends to be short-circuited by the GA sample. Furthermore, as expected, the GA sample partially

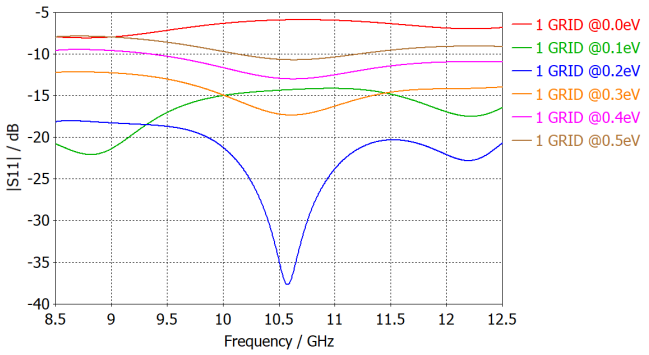


(a)

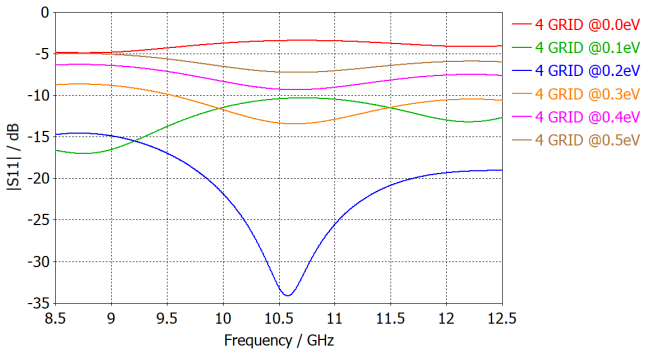


(b)

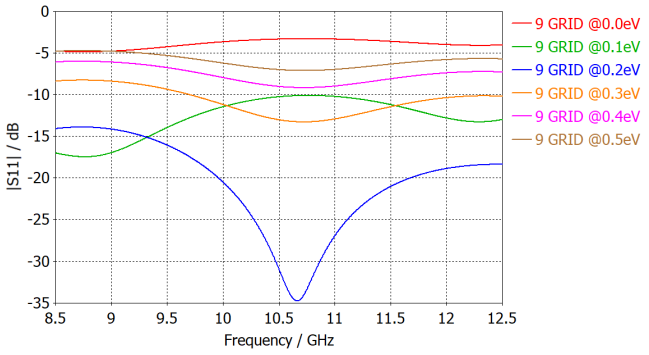


(c)

Fig. 4. Simulated reflection coefficient of the designed sensor for three different scenarios. The overall GA thickness is equal to 100 µm in (a), 400 µm in (b) and 900 µm in (c). To simulate the absorption gaseous molecules by GA sample, a sweep of the chemical potential from 0.0 eV to 0.5 eV with steps of 0.1 eV was performed for all scenarios.

absorbs the $TE_{10}$ mode. The trend observed is non-trivial but consistent across all the thicknesses considered. The amplitude consistently increases as the chemical potential increased from 0.0 eV to 0.2 eV and decreases when the chemical potential is further increased from 0.2 eV to 0.5 eV. Moreover, when the derivative of $S_{11}$ amplitude changes at 0.2 eV, the concavity of the frequency sweep is inverted. This combined effect shows that the sensor is capable of identifying small variations of chemical potential, representing a proof-of-concept demonstration that the proposed sensor can be a novel metrological tool for breath analyses. Fig. 4(a-c) shows the simulated reflection coefficient obtained for the same three total thicknesses of the graphene aerogel (1, 4 and 9 grids) while the chemical potential was varied from 0.0 eV to 0.5 eV. Experimental implementations of the proposed device are ongoing.

## V. Conclusions

We designed and simulated a sensor for breath analysis by integrating graphene aerogels of different thicknesses within rectangular waveguides having suitable gas inlet and outlet. We investigated the device using CST Studio Suite 2021 at frequencies $8 \div 12$ GHz, showing that small changes in chemical doping in the graphene aerogel are reflected in the transmission parameters of the waveguide. At first, we studied the effect of the aerogel thickness on the transmission coefficient, identifying optimal thickness. Then, we investigated the effect of chemical doping on devices having different aerogel thicknesses, showing good sensitivity to small changes in doping and non-trivial trends in the transmission parameters as a function of graphene chemical potential. The proposed structure represents a proof-of-concept for the use of graphene aerogels as a novel metrological tool for microwave gas sensors to be used for breath analysis. The design, here implemented using rectangular waveguides, can readily be modified to enable integration in miniaturized sensors.

## References


[1] *"Breath Biopsy-The complete Guide"*, Owlstone Medical LTD, Cambridge, UK.

[2] C. Lourenço, C. Turner, *"Breath Analysis in Disease Diagnosis: Methodological Considerations and Applications"*, Metabolites, June 2014.

[3] W. Ibrahim *et al.*, *"Diagnosis of COVID-19 by exhaled breath analysis using gas chromatography-mass spectrometry."*, ERJ Open Research 7, 2021.

[4] O. A. Ajbola *et al.*, *"Effects of dietary nutrients on volatile breath metabolites"*, Journal of Nutritional Science, vol. 2, 2013.

[5] A. S. Tahota *et al.*, *"A simple breath test for tuberculosis using ion mobility: A pilot study"*, Tuberculosis (Edinb). 99 (2016) 143–146.

[6] J. Taucher *et al.*, *"Detection of isoprene in expired air from human subjects using proton-transfer-reaction mass spectrometry."*, Rapid Commun Mass Spectrom., 1997.

[7] P. Spanel, D. Smith, *"Selected ion flow tube mass spectrometry analyses of stable isotopes in water: isotopic composition of H3O+ and H3O+ (H2O)3 ions in exchange reactions with water vapor."*, J Am Soc Mass Spectrom, 2000 Oct.

[8] D. Smith *et al*, *"Mass spectrometry for real-time quantitative breath analysis"*, Journal of Breath Research, vol. 8, no. 2, March 2014.

[9] C. Di Natale, R.Paolesse, E. Martinelli, R.Capuanoa, *"Solid-state gas sensors for breath analysis: A review"*, Analytica Chimica Acta, Volume 824, 8 May 2014, Pages 1-17.

[10] U. Tisch *et al.*, *"Detection of Asymptomatic Nigrostriatal Dopaminergic Lesion in Rats by Exhaled Air Analysis Using Carbon Nanotube Sensors"*, ACS Chemical Neuroscience, 3 (2012), pp. 161-166.

[11] K. Wlodzimirow *et al.*, *"Exhaled breath analysis with electronic nose technology for detection of acute liver failure in rats"*, Biosensors and Bioelectronics, 53 (2014), pp. 129-134.

[12] K. de Heer *et al.*, *"Electronic nose technology for detection of invasive pulmonary aspergillosis in prolonged chemotherapy-induced neutropenia: A proof-of-principle study"*, Journal of Clinical Microbiology, 51 (2013), pp. 1490-1495.

[13] C. Di Natale *et al.*, *"Lung cancer identification by the analysis of breath by means of an array of non-selective gas sensors"*, Biosensors and Bioelectronics, 18 (2003), pp. 1209-1218.

[14] M. Santonico *et al.*, *"In situ detection of lung cancer volatile fingerprints using bronchoscopic air-sampling"*, Lung Cancer, 77 (2012), pp. 46-50.

[15] P. Montuschi *et al.*, *"Diagnostic Performance of an Electronic Nose, Fractional Exhaled Nitric Oxide, and Lung Function Testing in Asthma"*, Chest, 137 (2010), pp. 790-796.

[16] J. A. Covington *et al.*, *"The application of FAIMS gas analysis in Medical Diagnostics"*, The Analyst 140(20), July 2015.

[17] R. P. Arasaradnam *et al.*, *"Non-invasive exhaled volatile organic biomarker analysis to detect inflammatory bowel disease (IBD)"*, Alimentary Tract, vol. 48, issue 2, pp. 148-153, February 01, 2016.

[18] G. Guarin, M. Hofmann, J. Nehring, R. Weigel, G. Fischer and D. Kissinger, *Miniature Microwave Biosensors: Noninvasive Applications*, IEEE Microwave Magazine, vol. 16, no. 4, pp. 71-86, May 2015.

[19] D. Zhi *et al.*, *A review of three-dimensional graphene-based aerogels: Synthesis, structure and application for microwave absorption*, Composites Part B: Engineering, Volume 211, 15 April 2021.

[20] E. Barrios *et al.*, *Nanomaterials in Advanced, High-Performance Aerogel Composites: A Review*, Polymers 2019, 11, 726.

[21] S. Turner *et al*, *"Boron Doping and Defect Engineering of Graphene Aerogels for Ultrasensitive NO2 Detection"*, J. Phys. Chem. C., June 2018.

[22] Y. Qian, I. M. Ismail, A. Stein, *"Ultralight high-surface-area, multifunctional graphene-based aerogels from self-assembly of graphene oxide and resol"*, Carbon, vol. 68, pp. 221-231, March 2014.

[23] R. Kubo, *"Statistical-Mechanical Theory of irreversible processes. I. General Theory and Simple Applications To Magnetic and Conduction Problems."*, Journal of the Physical Society of Japan, vol. 12, no. 6, June 1957.

[24] S. A. Awan *et al*, *"Transport conductivity of graphene at RF and microwave frequencies"*, 2D Materials, vol. 3, no.1, 2016.

[25] M. Bozzi, L. Pierantoni, S. Bellucci, *"Applications of Graphene at Microwave Frequencies"*, Radio Engineering, vol. 24, no. 3, September 2015.

[26] G. W. Hanson, *"Dyadic Green's Functions and guided surface waves for a surface conductivity model of graphene"*, Journal of Applied Physics 103, 2008.

[27] J. Zhang, W. Zhu, *"Graphene-Based Microwave Metasurfaces and Radio-Frequency Devices"*, Adv. Photonics Res., 2, 2021.

[28] H. Lee, K. Paeng, I. S. Kim, *"A review of doping modulation in graphene"*, Synthetic Metals 244(2018) 36-47.

[29] G. Zamiri, A. S. M. A. Haseeb, *"Recent Trends and Developments in Graphene/Conducting Polymer Nanocomposites Chemiresistive Sensors"*, Materials, July 2020.

[30] F. Schedin *et al*, *"Detection of Individual Gas Molecules Adsorbed on Graphene"*, Nature Mater, 2007.

[31] Zhu-Yin Sui *et al*, *"Nitrogen-Doped Graphene Aerogels as Efficient Supercapacitor Electrodes and Gas Adsorbents"*, ACS Appl. Mater. Interfaces 2015, 7, 1431-1438.

[32] A. K. Singh et al., *"Electrically tunable molecular doping of graphene,"* Applied Physics Letters, vol. 102, no. 4, 2013

[33] S. Janfaza *et al*, *"Digging deeper into volatile organic compounds associated with cancer"*, Bio. Meth. Prot., 2019.